

CLIO accelerator simulation in ASTRA

This report present simulation of CLIO accelerator in ASTRA code. Main parameters are summarised. To optimize bunch length study of phase is done.

The program ASTRA tracks particles through user defined external fields tacking into account the space charge field of the particle bunch. The tracking is based on a non-adaptive Runge-Kutta integration of 4th order [1]

Magnetic fields

To keep particles on orbit, several solenoids and quadruples was installed. Field of magnets is increased according to increase of particles energy. For low energy solenoids are fine, but for high energies quadruples are more applicable. For ASTRA simulation longitudinal on-axis field B_z is important. The transverse field components is calculated from the derivatives of the on-axis field [1]. To calculate on-axis field next formula is used [2]:

$$B_z = \frac{\mu n i}{2} \left[\frac{\xi}{\sqrt{\xi^2 + a^2}} \right]_{\xi_-}^{\xi_+}$$

where $\xi_{\pm} = z \pm \frac{L}{2}$, μ – permeability, a – coil radius, L – coil length, n – number of turns per unit lenght, i – current in each filament.

In script file of ASTRA this field is renormalized by maximum value given in [3].

Example of solenoid fields are presented on fig. 1

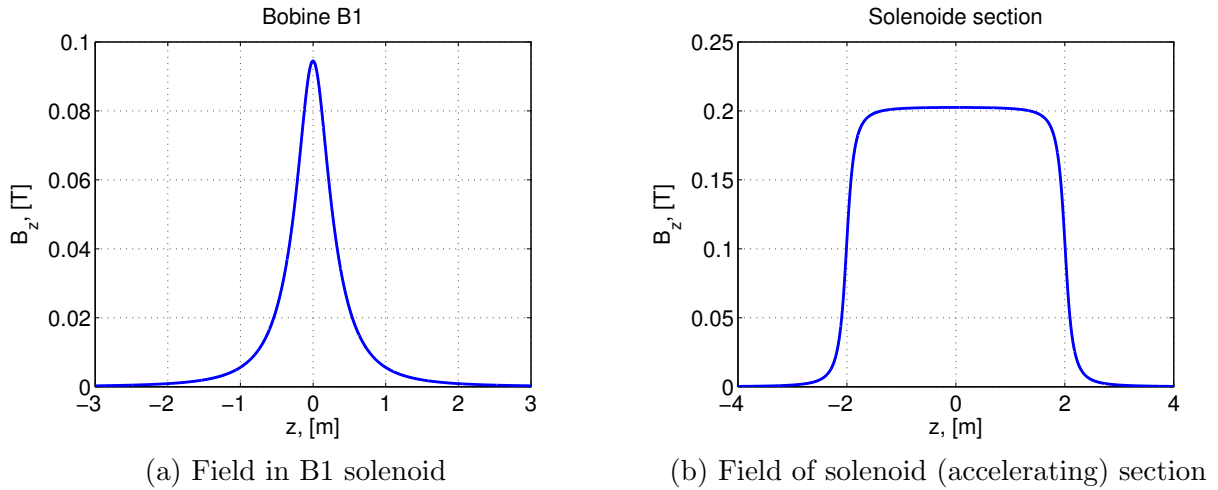
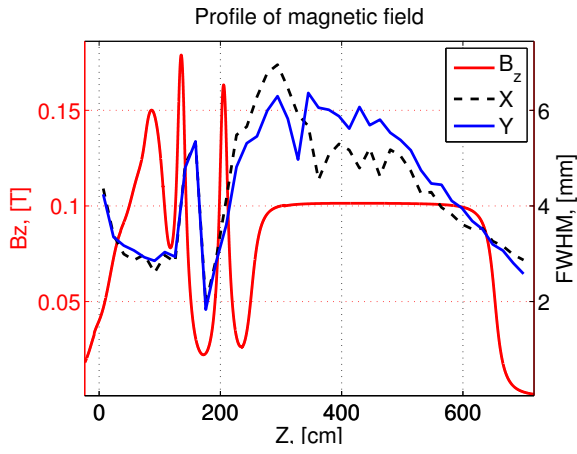
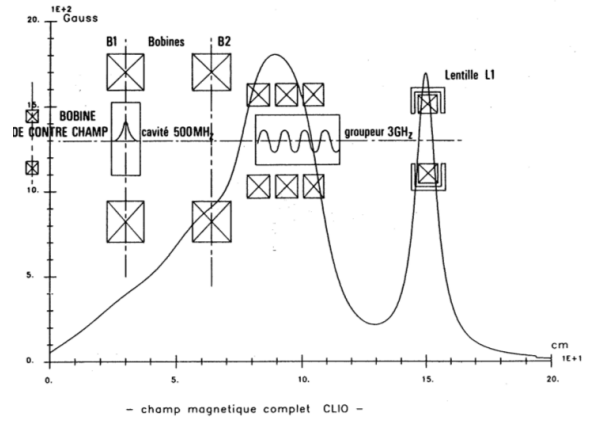


Figure 1: Examples of field in diiferent parts of CLIO accelerator

Quadruples are also present in CLIO accelerator, but they are out range of interest. Profile of magnetic field presented on fig 2, which is in agreement with previous calculation:



(a) Magnet field along the accelerator with transverse bunch width



(b) Magnet field along the accelerator [3]

Figure 2: Profile of magnetic field

Gun

The gun is a classical Pierce gridded gun with a thermoelectric dispenser cathode [4]. This gun have quite complicate geometry, so in ASTRA simulation was used simplified model of it with saving all out parameters (emittance, x-y distribution, bunch length, energy etc).

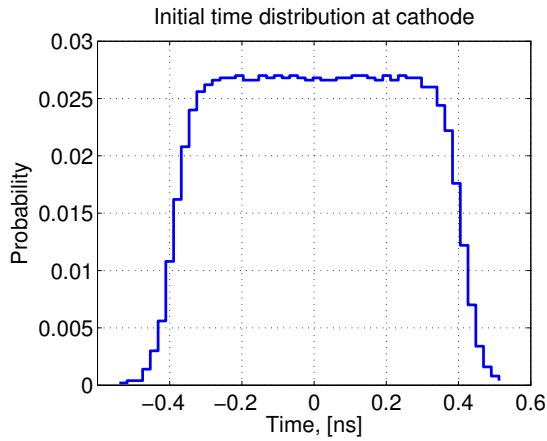
To generate initial distribution program generator is used (additional program to Astra). Main parameters are follow:

$Cathode=T$ – particles are emitted from cathode, so temporal distribution is generated rather than Z .

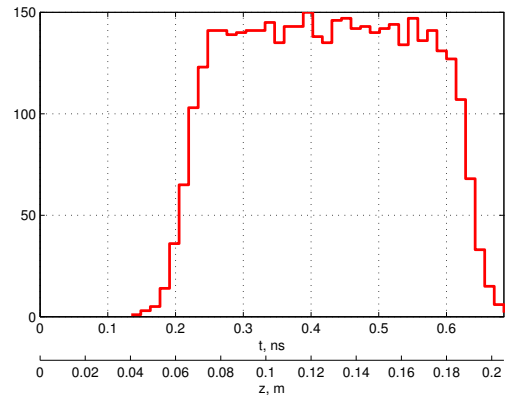
$Q_{total}=1.2E0$ – total charge is 1.2nC

$Dist_z='plateau'$, $Lt=0.8E0$, $rt=0.1E0$ – temporal distribution (see fig. 3) is plateau with length 0.8ns and rising edge 0.1 ns. P_z for all particles equal zero.

In XY plane particles are distributed by Gaussian distribution with sigma equal 2 mm.



(a) Time distribution at cathode



(b) Longitudinal distribution at exit of gun

Figure 3: Temporal distribution

Emittance is $15\pi mm \times mrad$

$Dist_x='gauss'$, $sig_x=2.0E0$

$Dist_px='g'$, $Nemit_x=15.0E0$,

Same set fot Y.

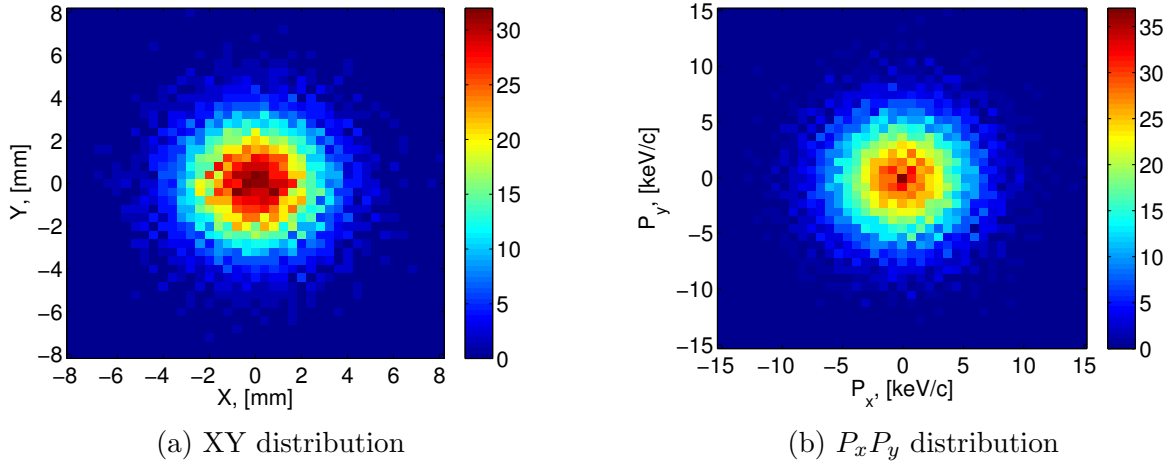


Figure 4: Distributions of particles at cathode

Parameter	Value	Source
Total charge (Q_{total})	1.2 nC	[6]
Emmission time (Lt)	0.9 ns	[4]
Cathode diameter	8 mm	[4]
Norm. emmitance	$15\pi mm \times mrad$	[4],[3],[5]
Energy of electrons	90 keV	[4],[5]
Cathode-Anode dist.	24 mm	[4],[5]

To simulate gun, cavity with dc field is created.

$FILE_EFieLD(1) = 'GUN.dat'$, $C_pos(1)=0$, $C_higher_order(1)=T$, $MaxE(1)=-3.75$, $Phi(1)=0.0$,

And at the exit of gun aperture with 8 mm diameter is installed

$\mathcal{E}APERTURE$

$LApert=T$,

$File_Aperture(1)='Rad'$, $Ap_Z1(1)=-0.001$, $Ap_Z2(1)=0.0$, $Ap_R(1)=4$, $!iris_des_canon$

/

Cross section of parameters exactly after aperture is not very informative as part of electrons still emitting from cathode. After aperture distributions presented on fig.5.

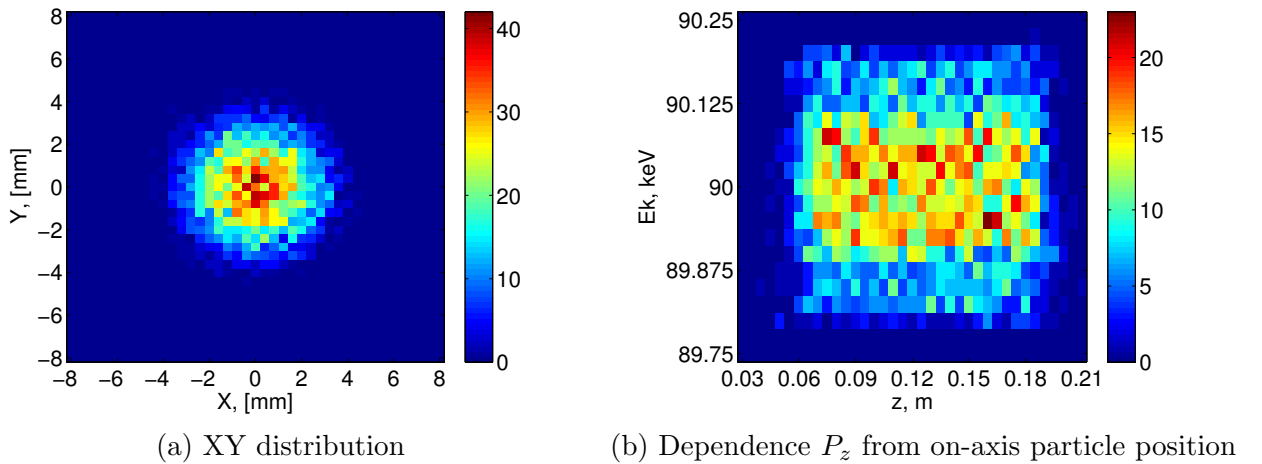


Figure 5: Distributions of particles after the gun

Bunching

Subharmonic buncher

The subharmonic buncher is a stainless-steel reentrant cavity in the mode TM01 at 499.758 MHz i.e. the 1/6th subharmonic of the fundamental frequency of the accelerating cavity [6].

Parameter	Value	Source
Height of the gap	19mm (18.6 mm)	[3] ([5] p.62)
Working frequency	499.758 MHz	[3] p.41
Voltage	30 kV	[3] p.39; [5] p.62
Phase	180 deg.	[4]
Mode	TM01	[3] p.39; [5] p.62
Bunch length before SGB	$\tilde{1}$ ns	[3] p.39
Bunch length after SGB	$\tilde{0.2}$ ns (180 ps)	[3] p.39 ([5] p.61)
Energy before FB	$\gamma = 1.195, \beta = 0.548$	[3] p.45
Pulse duration before FB	$i=200$ ps	[3] p.45
Energy spread FB	$\Delta\gamma/\gamma = 4.9e - 2$	[3] p.45

Important role in bunch compression play correct phase and maximum field of the cavity. So 2D scan is required. Main criterion is to get bunch optimal for further bunching and acceleration. On figure 6 presented amplitude of the bunch, FWHM, FW0.1M and relative velocity (β) as function of phase and field amplitude.

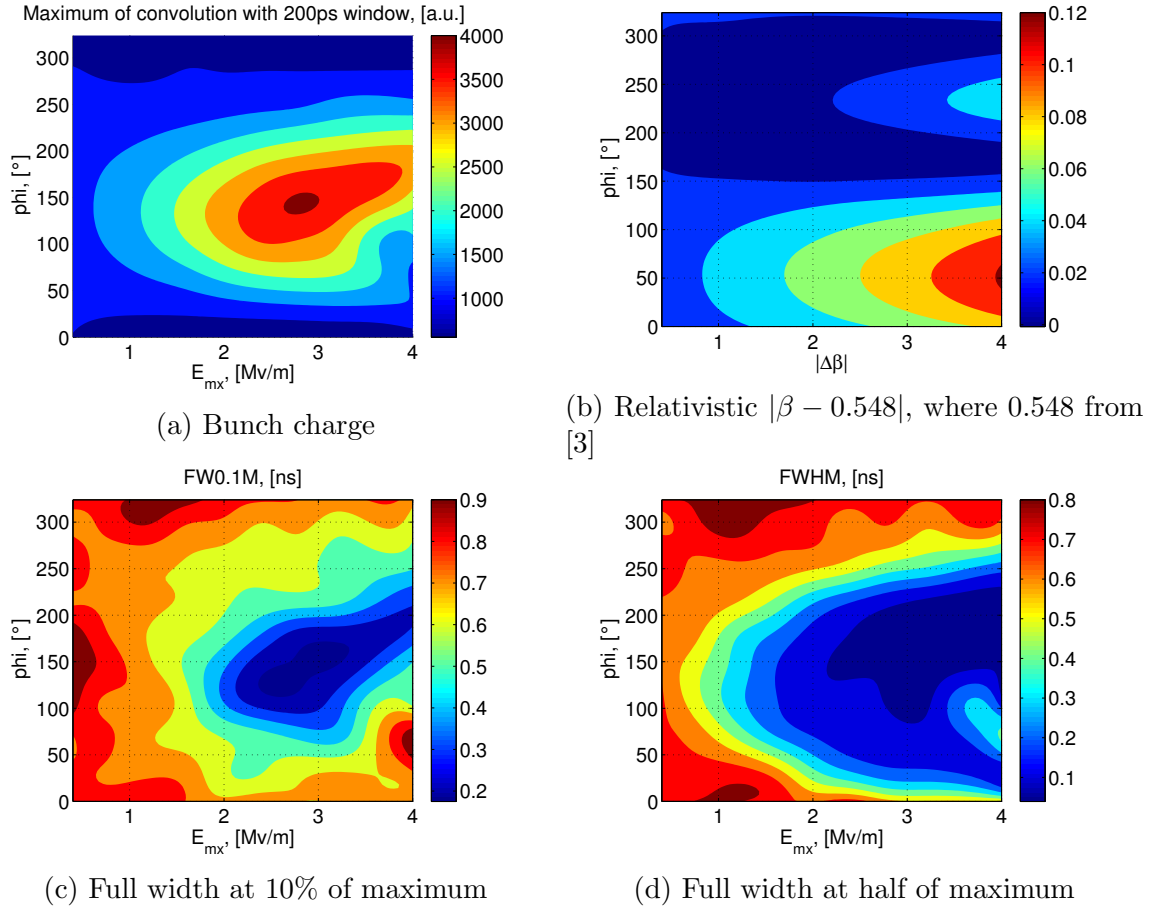
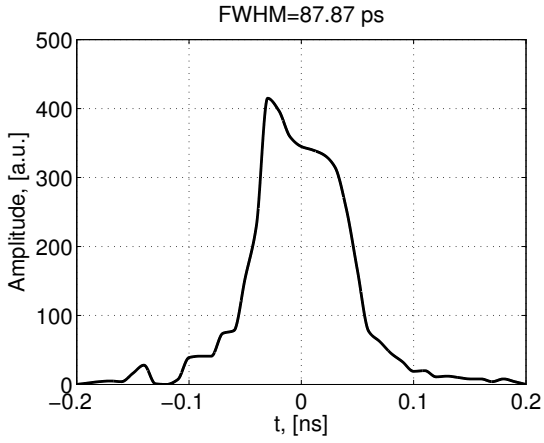


Figure 6: Dependence of bunch parameters from phase and field amplitude

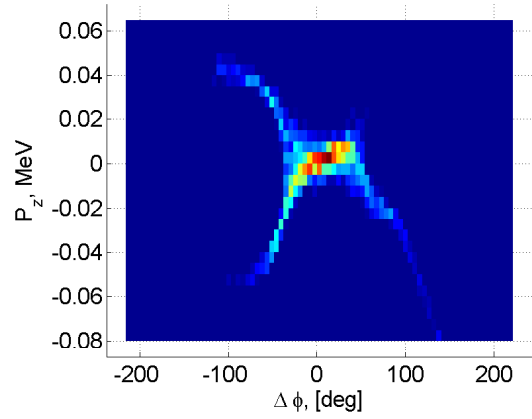
As there are several parameters by which bunches are selected (fwhm, fw0.1m, amplitude etc), so there is need to maximise amplitude and minimise bunch width. Big fw0.1m (long tails) will produce satellites. So I choose minimum of fw0.1m, which is close to maximum of

amplitude and minimum of fwhm. All measurements are made at the entrance of fundamental buncher. So the phase is 126 degree and field is 2.56 MV/m.

So at phase of 126 degree bunch distribution is presented on fig. 7



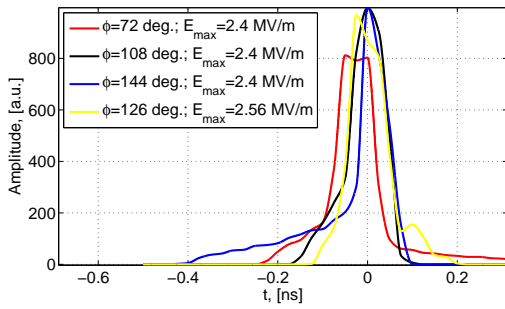
(a) Longitudinal distribution



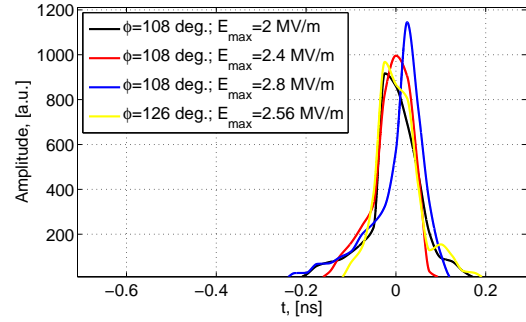
(b) P_z vs. $\Delta\phi$ distribution (according to reference particle)

Figure 7: Distributions of bunch at entrance of FSW buncher

Bunch distribution near working point is presented on fig.8.



(a) Longitudinal distribution with varying phase



(b) Longitudinal distribution with varying field

Figure 8: Longitudinal distribution of bunch near working point

Fundamental buncher

The fundamental buncher is a copper triperiodic, S-band standing wave structure. It is composed of 3 wavelength, slightly matched to the beam velocity (0.92, 0.98 and 1 lambda) of the buncher [7]. The role of the 3 GHz buncher is to complete the compression phase current pulses initiated by the cavity subharmonic 500 MHz and also to give the micro-particles pack enough energy to make them ultrarelativistic [3].

On figure 9 field in fundamental buncher is presented. It is used in ASTRA simulation and field of this buncher from [3].

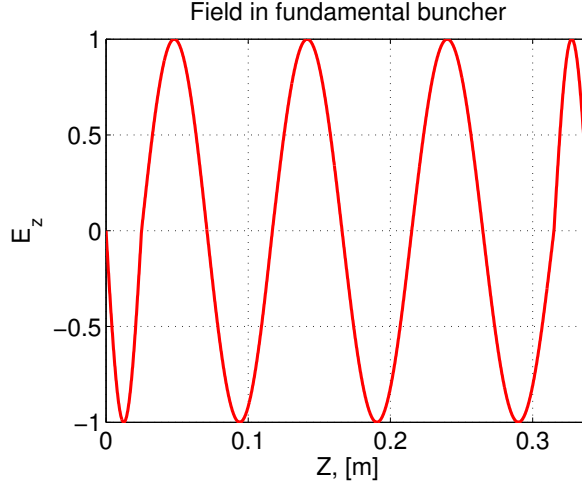
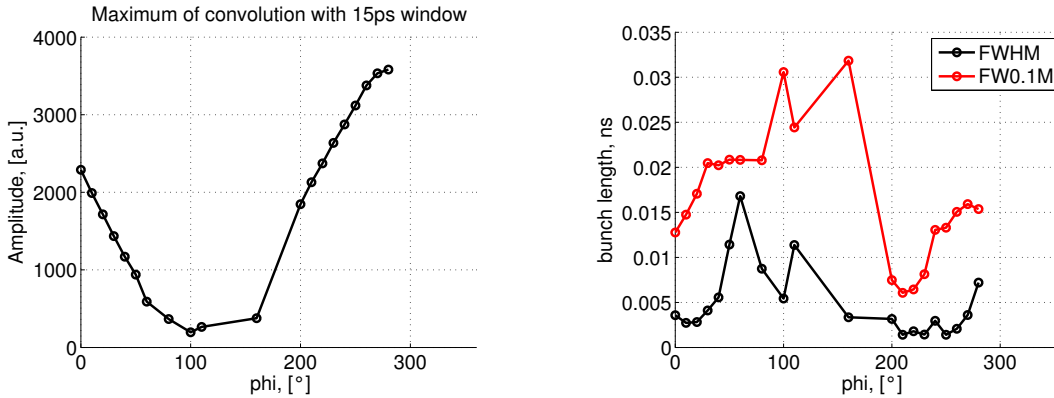


Figure 9: Field in fundamental buncher

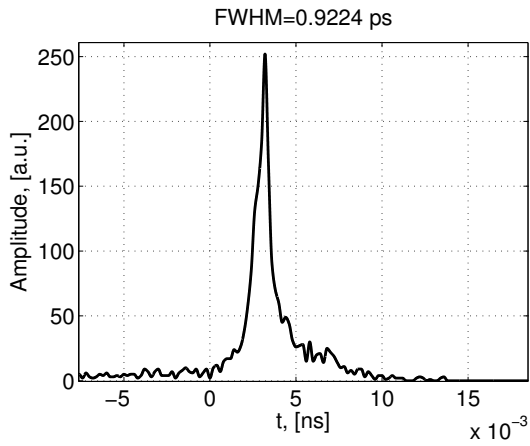
Parameter	Value	Source
λ_0	10 cm	[3] p.45
Frequency	2998.55 MeV	[3] p.45
No load energy	4 MeV	[3] p.46; [7]
Useful length	0.35 m	[7];[6]
dE/dz	22 MeV/m	[6]
Out energy	≥ 2.84 MeV	[3] p.53
Out pulse width	≤ 15 ps	[3] p.53

As subharmonic buncher, fundamental buncher also require phase study. On fig. 10 are presented most important results.

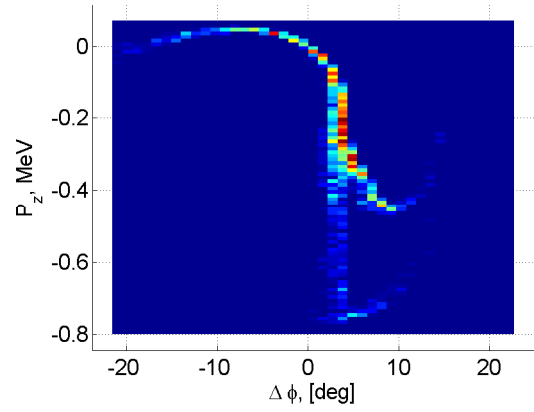


(a) Dependence of bunch amplitude from phase of FSW buncher
 (b) Dependence of full width at half and 10% of maximum from phase of cavity

Figure 10: Phase study plots for FSW buncher



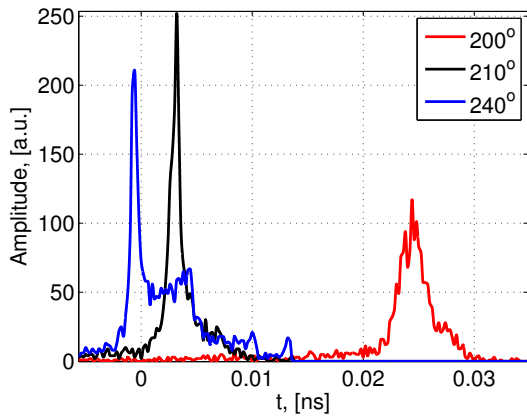
(a) Longitudinal distribution of bunch



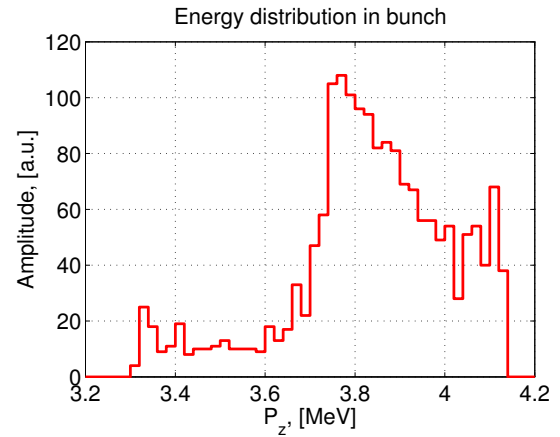
(b) P_z vs. z distribution of bunch

Figure 11: Distributions of bunch at entrance of accelerating cavity for phase of FSW buncher 210 degree

For this case most applicable phase is 210 degree. On fig 11 bunch distribution is presented. If reader is curious in energy distribution of resulted bunch, he can find answer on fig. 16b. For this subsection all distribution are taken at the entrance of accelerating cavity.



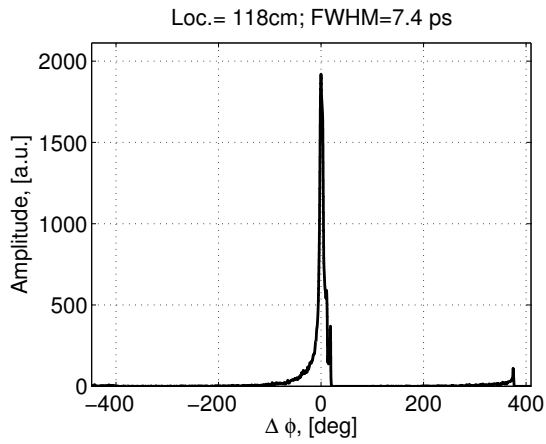
(a) Longitudinal distribution of bunch near working point



(b) Energy distribution in bunch

Comparison with PARMELA

For this subsection all distributions are taken at the exit of fundamental buncher.



(a) Longitudinal distribution of bunch

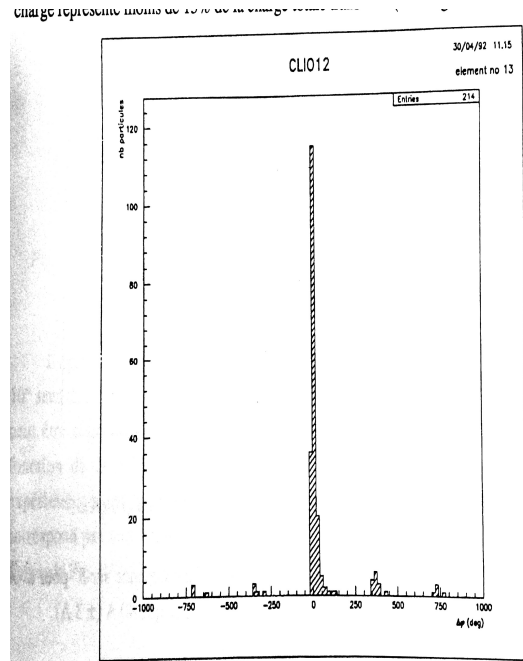
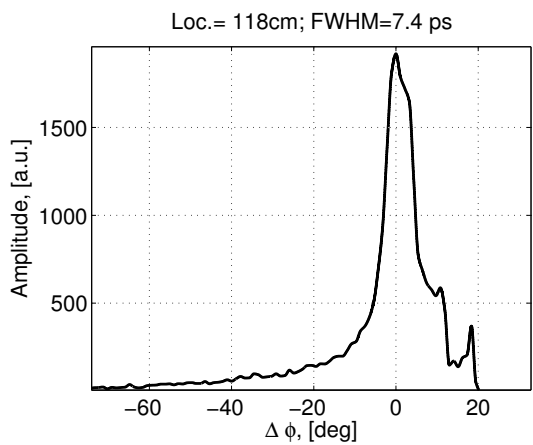


Fig. IV-3: En sortie du groupeur, le paquet principal est entouré de petits paquets satellite. Leur charge représente moins de 15% de la charge totale transmise.

(b) ...



(a) Longitudinal distribution of bunch

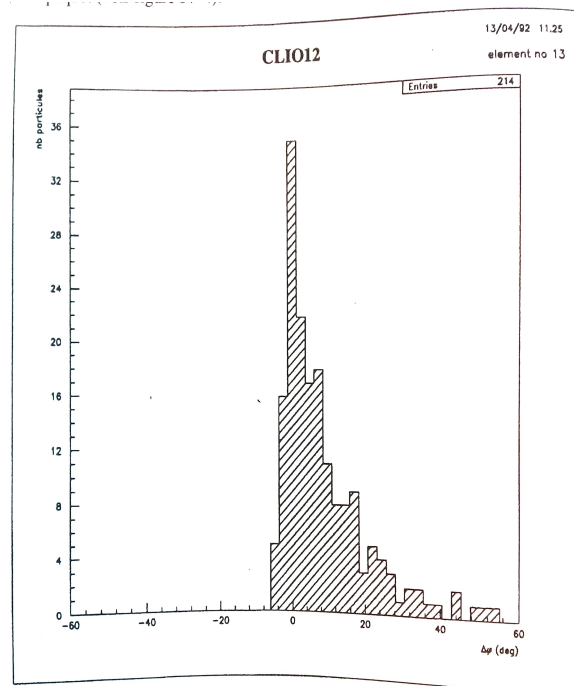
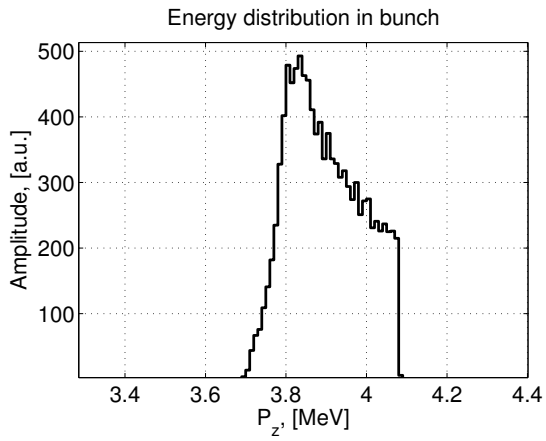


Fig. IV-4: Profil longitudinal d'un paquet d'électrons en sortie du groupeur.

(b) ...



(a) Longitudinal distribution of bunch

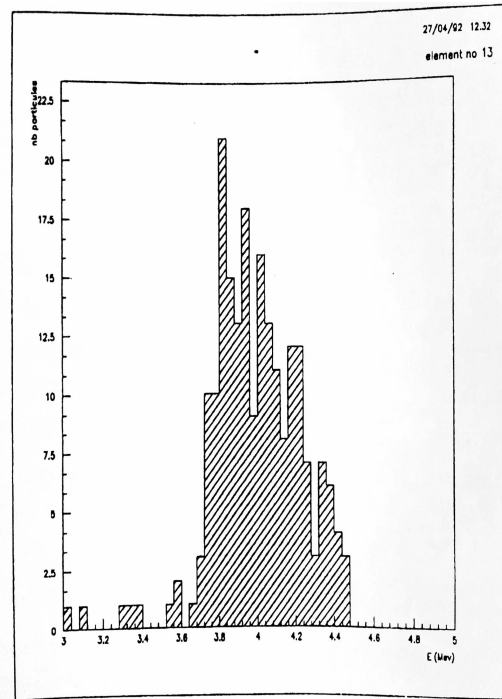
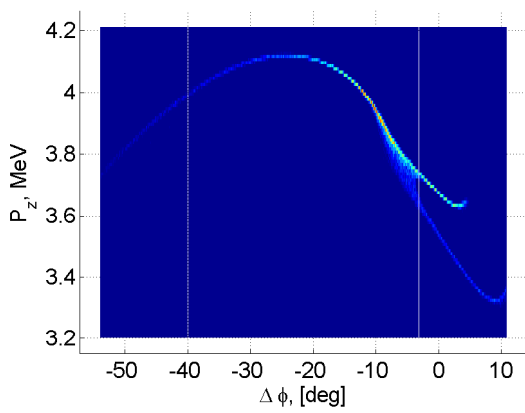


Fig. IV-7: Spectre en énergie en sortie du groupeur, d'après PARMELA.

(b) ...



(a) Longitudinal distribution of bunch

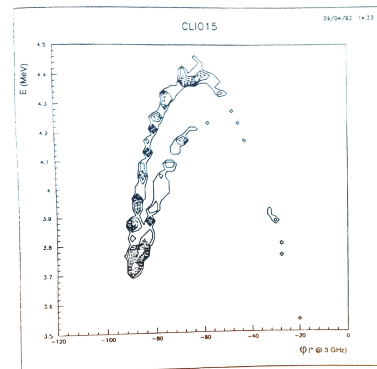


Fig. IV-8: Diagramme phase-énergie en sortie du groupeur d'après PARMELA, lorsque l'on minimise la largeur des paquets.

(b) ...

The accelerating cavity

The cavity is a constant gradient S band travelling wave disk-loaded structure. The cavity is surrounded with a set of solenoidal coils which give a continuous axial field adjustable up to 0.2 Tesla [7].

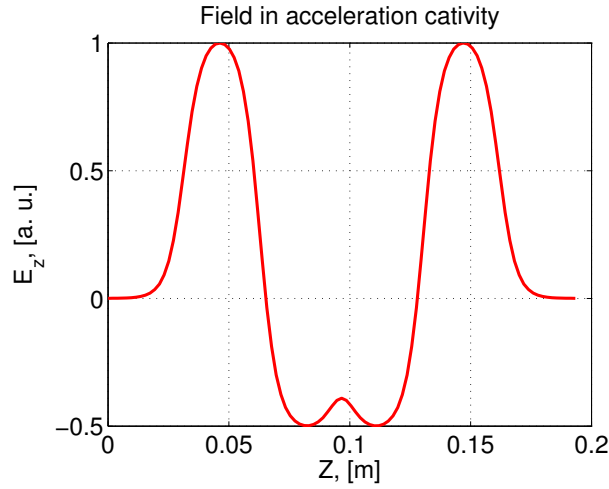


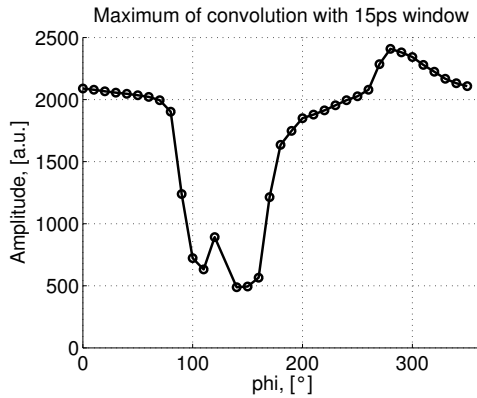
Figure 17: Field in accelerating cavity (field amplitude of one RF period plus the input and output coupler cells)

Parameter	Value	Source
frequency	2998.550	[7]
length	4.5m	[7]
mode	$2\pi/2$	[7]
no load energy	78 MeV	[7]
cell number	135	[3]

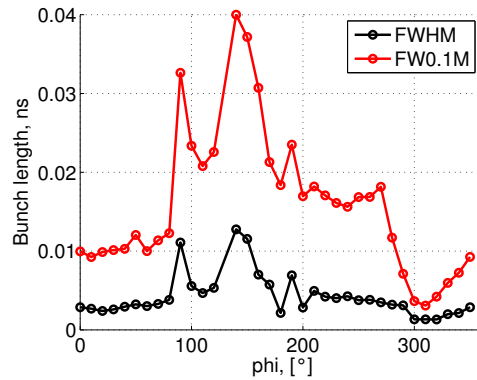
Same phase study are done for accelerating cavity.

Maximum field in cavity is 22 MV/m. Phase 310 degree give smallest bunch length (fig. 18b), but energy spread for it is quite big (fig. 18e), so phase 20 degree is choosen. Distribution of bunch is presented on figure 19.

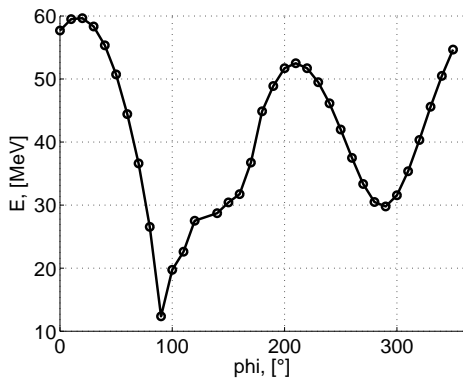
Spectrum of the profile presented on figure 22.



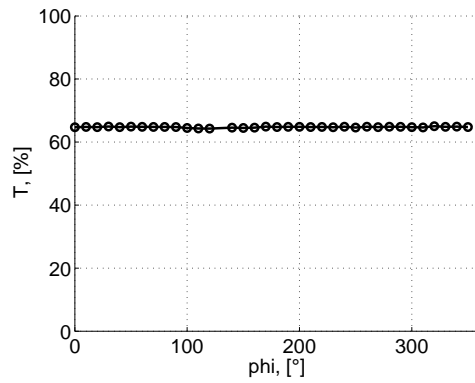
(a) Dependence of bunch amplitude from phase of accelerating cavity



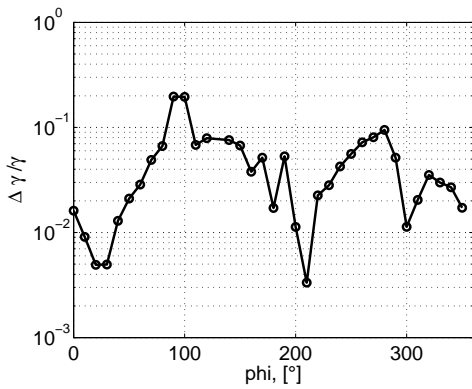
(b) Dependence of the full width at half and 10% of maximum from phase of cavity



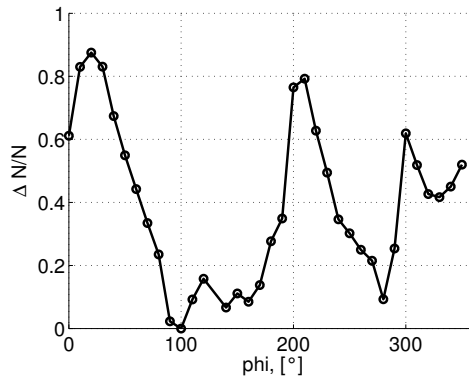
(c) Dependence of the bunch energy from phase of accelerating cavity



(d) Dependence of the transmission from phase of cavity

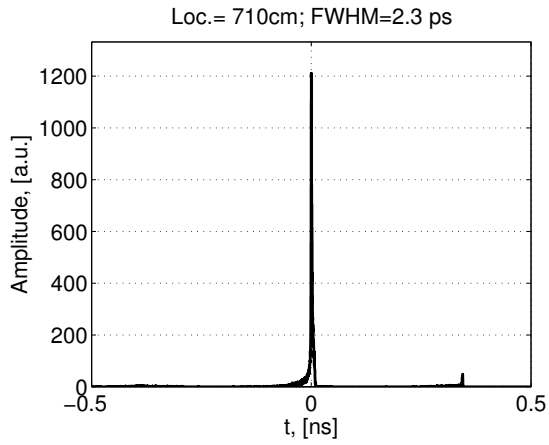


(e) Dependence of the bunch energy spread from phase of accelerating cavity

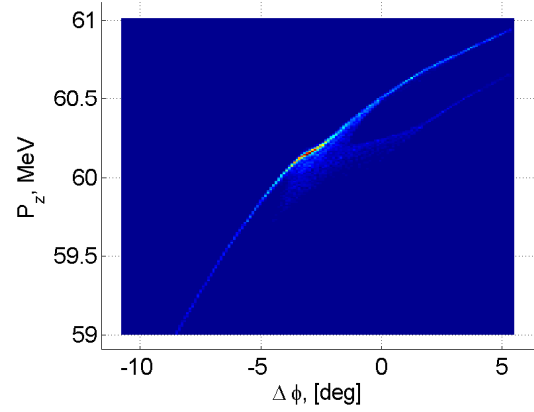


(f) Dependence of the number of particles in bunch 2% energy spread to number of particles in bunch from phase of the cavity

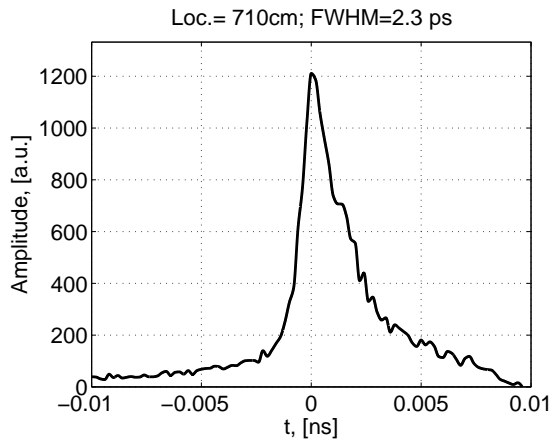
Figure 18: Phase study plots for accelerating cavity



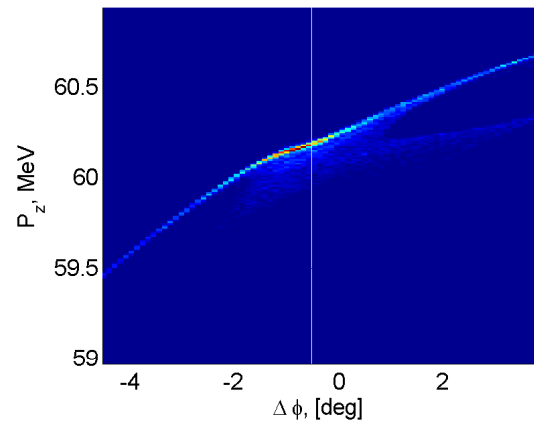
(a) Longitudinal distribution of bunch



(b) P_z vs. t distribution of bunch

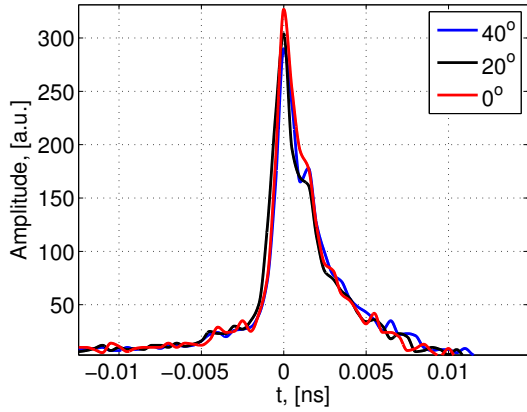


(c) Longitudinal distribution of bunch (zoomed)

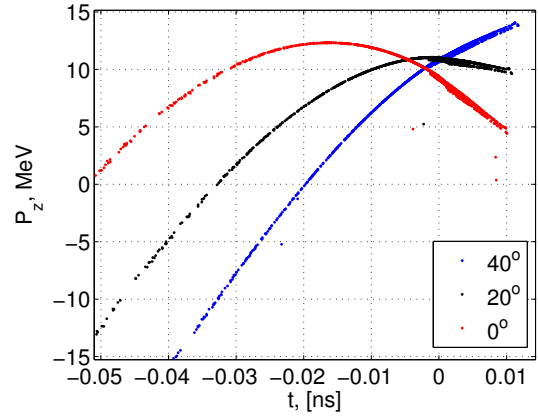


(d) P_z vs. t distribution of bunch (zoomed)

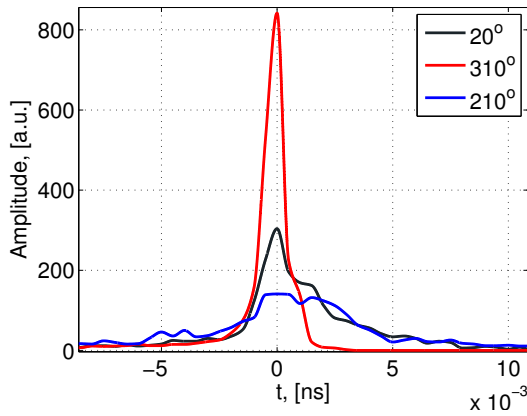
Figure 19: Distributions of bunch at the exit of accelerating cavity for 20 degree phase



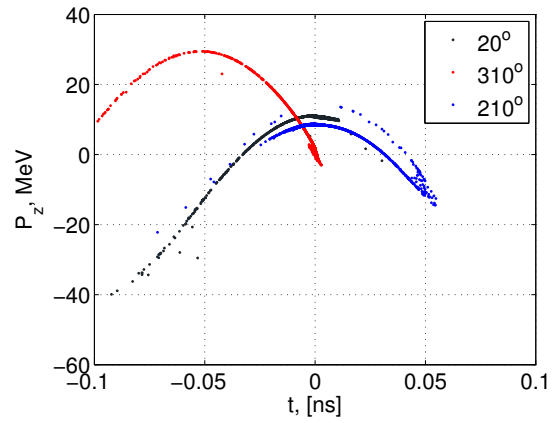
(a) Longitudinal distribution of bunch



(b) P_z vs. t distribution of bunch

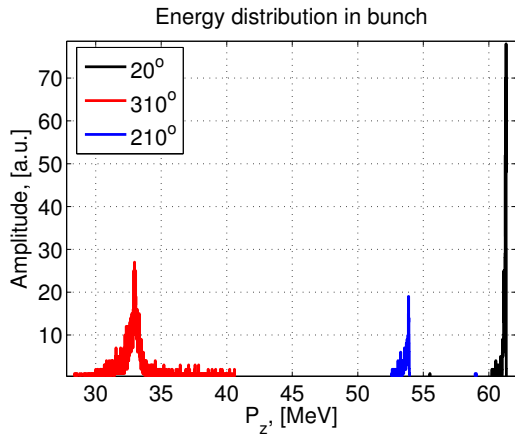


(c) Longitudinal distribution of bunch

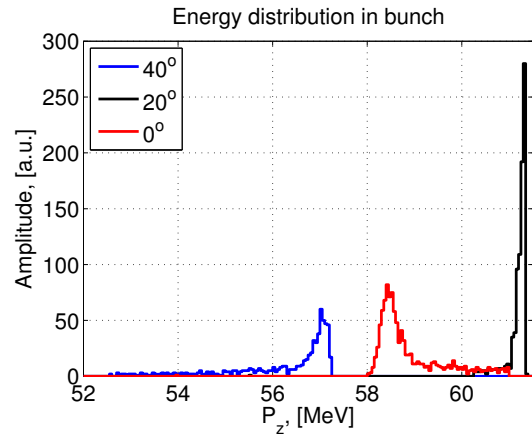


(d) P_z vs. t distribution of bunch

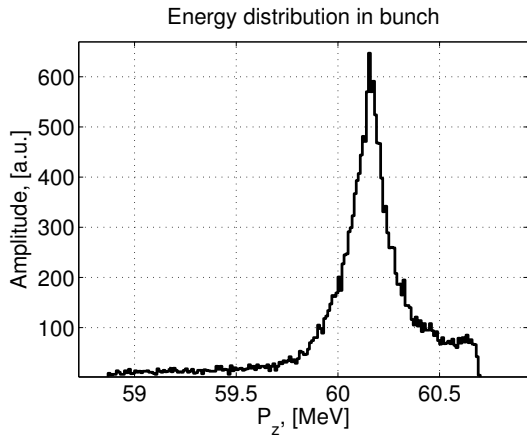
Figure 20: Distributions of bunch at the exit of accelerating cavity for 3 phases



(a) Energy distribution of bunches



(b) Energy distribution of bunches



(c) Energy distribution of bunch

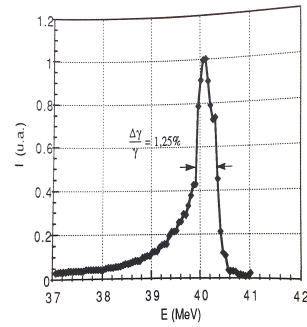
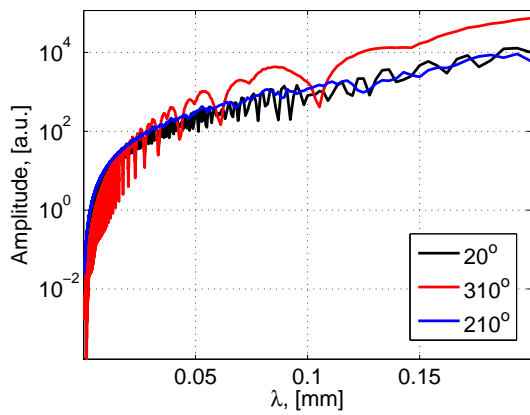


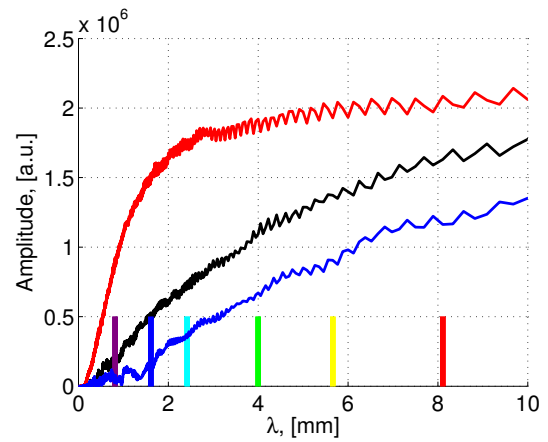
Fig. IV-9: Spectre en énergie à 40 MeV, tir du 02/10/92. Après déconvolution, la dispersion est ici estimée à 1%.

(d) PARMELA [5]

Figure 21: Distributions of bunch at the exit of accelerating cavity

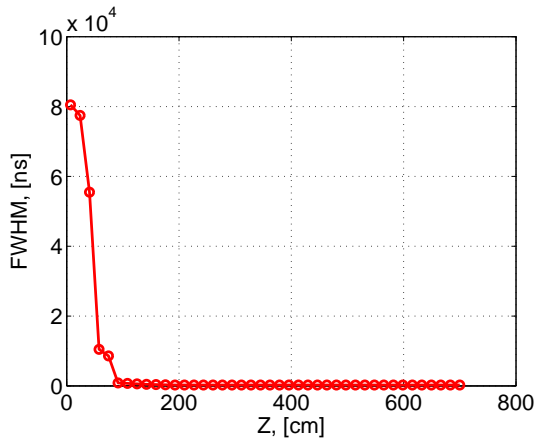


(a) Spectrum of profile in (0,0.2)mm region

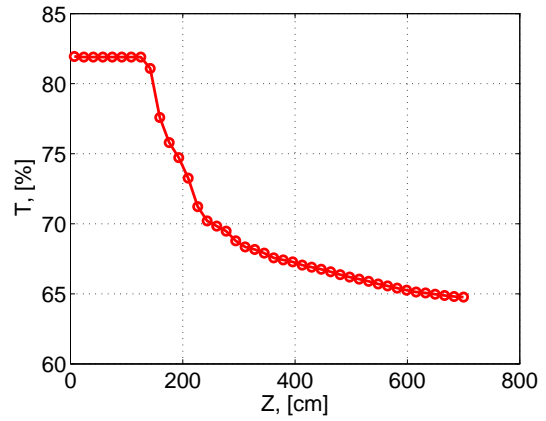


(b) Spectrum of profile in (0,10)mm region

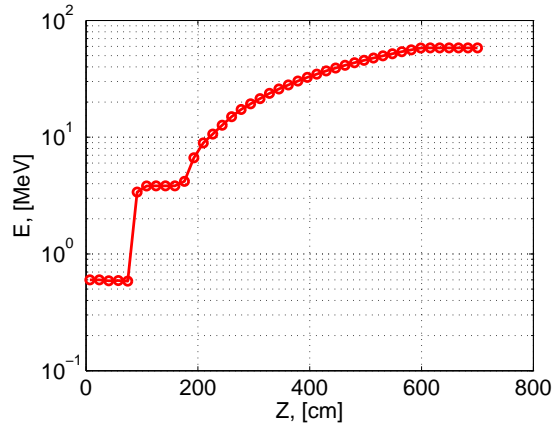
Figure 22: Spectrum of profile (Black – 20°, Red – 310°, Blue – 210° phase)



(a) Dependence of the bunch width from distance in accelerator



(b) Dependence of the transmissivity from distance in accelerator



(c) Dependence of the bunch energy from distance in accelerator

Figure 23: Some dependences from distance

Bibliography

- [1] Klaus Floettmann, *A Space Charge Tracking Algorithm Version 3.0*, DESY, Germany, October 2011(Update April 2014)
- [2] Edmund E. Callaghan, Stephen H. Maslen *NASA Technical note D-465. The magnetic field of finite solenoid*, Washington, USA, October 1960
- [3] *Rapport d'étude du projet de laser a electrons libres sur accelerateur lineaire HF 3 GHz: CLIO*,LAL/RT-89/04
- [4] J.C.Bourdon & comp. *Commissioning the CLIO injection system*, NIMPR A305(1991) 322-328
- [5] Francois GLOTIN *Le laser a electrons libres CLIO et sa structure temporelle* These, Univ. Paris VII, 1994
- [6] R. Chaput & comp. *Optimisation of the FEL CLIO Linear Accelerator*
- [7] J.C.Bourdon & comp. *CLIO: Free Electron Laser in ORSAY*